ResearchGate

See discussions, stats, and author profiles for this publication at: https://www.researchgate.net/publication/238940983

A study of field induced transitions (FiT) in the nematic phase of an inter hydrogen bonded ferroelectric liquid crystal

ARTICLE *in* SOLID STATE SCIENCES · APRIL 2010

Impact Factor: 1.84 · DOI: 10.1016/j.solidstatesciences.2009.12.012

CITATIONS
13

READS
18

2 AUTHORS:

Vijayakumar V N
Bannari Amman Institute of Technology
30 PUBLICATIONS **325** CITATIONS
SEE PROFILE

M. L. N. Madhu Mohan
Bannari Amman Institute of Technology
85 PUBLICATIONS **624** CITATIONS
SEE PROFILE

Available from: M. L. N. Madhu Mohan
Retrieved on: 25 January 2016

Provided for non-commercial research and education use.
Not for reproduction, distribution or commercial use.

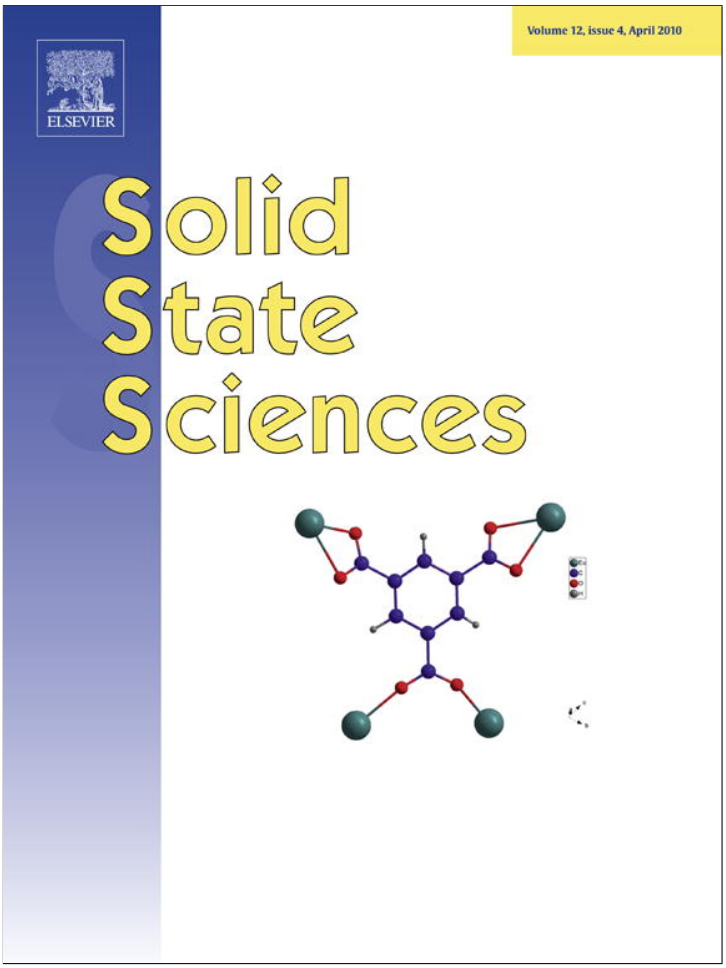

This article appeared in a journal published by Elsevier. The attached copy is furnished to the author for internal non-commercial research and education use, including for instruction at the authors institution and sharing with colleagues.

Other uses, including reproduction and distribution, or selling or licensing copies, or posting to personal, institutional or third party websites are prohibited.

In most cases authors are permitted to post their version of the article (e.g. in Word or Tex form) to their personal website or institutional repository. Authors requiring further information regarding Elsevier's archiving and manuscript policies are encouraged to visit:

http://www.elsevier.com/copyright

Author's personal copy

Solid State Sciences 12 (2010) 482–489

Contents lists available at ScienceDirect

Solid State Sciences

journal homepage: www.elsevier.com/locate/ssscie

A study of field induced transitions (FiT) in the nematic phase of an inter hydrogen bonded ferroelectric liquid crystal

V.N. Vijayakumar, M.L.N. Madhu Mohan*

Liquid Crystal Research Laboratory (LCRL), Bannari Amman Institute of Technology, Sathyamangalam, Tamilnadu 638 401, India

ARTICLE INFO

Article history:
Received 9 September 2009
Received in revised form
10 December 2009
Accepted 14 December 2009
Available online 23 December 2009

Keywords:
Liquid crystals
Chemical synthesis
Dielectric response
Field induced transition

ABSTRACT

A novel series of hydrogen bonded ferroelectric liquid crystals (HBFLC) have been isolated. Hydrogen bond is formed between non mesogen chiral ingredient (S)-1, 2–cholo-3-(4-hydroxy) phenyl propionic acid and mesogenic p-n alkoxy benzoic acids. Phase diagram is constructed from the transition temperatures obtained by differential scanning calorimetry (DSC) and polarizing optical microscopic (POM) studies. Thermal and electrical properties exhibited by a hydrogen bonded complex namely (S)-1,2–cholo-3-(4-hydroxy)phenyl propionic acid with octyloxy benzoic acid (CTy + 8BA) are discussed. Observation of dielectric hysteresis in CTy + 8BA makes it more suitable for device applications. Salient feature of the present work is observation of a field induced transitions in nematic phases pertaining to the above complex designated as FiT. This phenomenon has been confirmed by optical textures of POM, helicoidal measurements, optical intensity and dielectric studies. Four threshold electrical field values are noticed which in turn contributed to four new phases (E_1, E_2, E_3 and E_4) induced by electric field and helical pitch measurements supports the above observation. FiT is reversible in the sense that when applied field is removed the original texture is restored.

© 2009 Elsevier Masson SAS. All rights reserved.

1. Introduction

Kato reported [1] enhancement of the mesogenic range through the formation of inter molecular hydrogen bond between two dissimilar moieties. Different types of liquid crystalline structures are reported in literature [2–14] where in covalent bonds are the building blocks. In recent times [5–13,18–21], much work has been done on the molecular architecture through self assembly process in which hydrogen bonds play a pivotal role. Hydrogen bonding owes its importance because of its directionality and high stability. Many super molecular self assembly systems have been built [2,7,8] using hydrogen bonds which exhibited liquid crystallinity. The molecular reorganization process by a single hydrogen bond between mesogenic carboxylic acids and various non mesogenic compounds yielding a mesogenic hydrogen bonded complex are reported in the literature [5–12]. These inter molecular interactions increase the molecular aggregations. Kato and his group reported [2,7,8] that the magnitude and direction of hydrogen bonds determines the mesogenic range.

Liquid crystals with self organizing capability and with ferroelectric property, known as hydrogen bonded ferroelectric liquid crystals [HBFLC] are reported [2–14] widely in literature. These liquid crystals are designed and synthesized from materials selected on the basis of their molecular reorganization and self assembly capability. The applicational aspects [15–18], and commercial viabilities made many research groups to work on these hydrogen bonded ferroelectric liquid crystals.

Hydrogen bonded liquid crystalline materials are known since early 1960s [3,4], however in the recent times [5–13,18–21] much work has been done on these complexes. Hydrogen bond enables various mesogenic and non mesogenic compounds to form complexes which exhibit rich phase polymorphism. HBFLC usually are composed of a proton donor and acceptor molecules. The reported data [5–12,18–22] indicates the fact that if an HBLC material to be mesogenic it is enough either one of proton donor or an acceptor molecules exhibits mesogenic property. The chemical molecular structure [10,18–22] of HBFLC is co-related to the physical properties exhibited by it. The reported literature [13–21] suggests the formation of HBFLC through carboxylic acids as well as from mixtures of unlike molecules capable of interacting through H-bonding. Usually in all these HBLC the rigid core is made up of covalent and non covalent hydrogen bond. With our previous experience [23–30], in designing, synthesizing and characterizing various types of liquid crystals, a successful attempt has been made in characterizing a novel series of inter hydrogen bonded ferroelectric liquid crystal.

* Corresponding author. Tel.: +91 9442437480; fax +91 4295 223 775.
E-mail address: mln.madhu@gmail.com (M.L.N. Madhu Mohan).

1293-2558/$ – see front matter © 2009 Elsevier Masson SAS. All rights reserved.
doi:10.1016/j.solidstatesciences.2009.12.012

Author's personal copy

In the present communication a homologous series of HBFLC is designed in such a way that the molecule possesses a chiral center and the hydrogen bonding is on one side of the chiral centre moiety. (S)-1,2–cholo-3-(4-hydroxy) phenyl propionic acid is the ferroelectric ingredient formed hydrogen bond with mesogenic p-n alkoxy benzoic acid. Thermal and electrical characterization of one HFBLC complex of the present series is discussed in detail.

2. Experimental

Optical textural observations were made with a Nikon polarizing microscope equipped with Nikon digital CCD camera system with 5 mega pixels and 2560 × 1920 pixel resolutions. The liquid crystalline textures are processed, analyzed and stored with the aid of ACT-2U imaging software system. The temperature control of the liquid crystal cell is equipped by Instec HCS402-STC 200 temperature controller (Instec, USA) to a temperature resolution of ± 0.1 °C. This unit is interfaced to computer by IEEE –STC 200 to control and monitored the temperature. The liquid crystal sample is filled by capillary action in its isotropic state into a commercially available (Instec, USA) polyamide buffed cell with 4 micron spacer. Optical extinction technique is used for the determination of tilt angle. The transition temperatures and corresponding enthalpy values are obtained by DSC (Shimadzu DSC-60). FTIR spectra is recorded (ABB FTIR MB3000) and analyzed with the MB3000 software. The dc bias voltage is derived from Agilent HP4192A LF impedance analyzer. AC voltage is obtained from Tektronix AFG 3021B generator, it is amplified by an indigenous circuit comprising of a high voltage amplifier BB 3583. The p-n-alkoxybenzoic acids (*n*BA) and levo tyrosine are supplied by Sigma Aldrich, Germany and all the solvents used are E.Merk grade. The purity of octyloxy and nonyloxy benzoic acids are 98%, 97% respectively while the purity of levo tyrosine is 98%.

2.1. Synthesis of HBFLC

The synthetic route for preparation of (S)-1, 2–cholo-3-(4-hydroxy) phenyl propionic acid is given as Scheme 1 while a detailed synthetic procedure including various intermediates is presented below.

(S)-1,2–cholo-3-(4-hydroxy)phenyl propionic acid (**1**) is prepared by dissolving (S)-2–amino-3-(4-hydroxy)phenyl propionic acid (5.43 g, 30.0 mmol) in 20 cm^3 of 6 N HCl and the resulting solution is maintained between 0 °C and 5 °C. Freshly pulverized sodium nitrite (2.72 g, 32.0 mmol) is added to the solution in small portions with vigorous stirring while maintaining the reaction temperatures between 0 °C and 5°C. The reaction mixture is stirred for 12 h and then extracted with 40 cm^3 of diethyl ether. The ethereal layer is dried over anhydrous sodium sulphate for 12 h. The crude yellow product obtained on removing the excess solvent by distillation under reduced pressure, is washed repeatedly with cold EtOH and finally recrystallized from hot dichloromethane to get 55% yield.

Intermolecular hydrogen bonded ferroelectric mesogens are synthesized by the addition of 1 mol of p-n-alkoxybenzoic acids with 1 mol of above synthesized (S)-1,2–cholo-3-(4-hydroxy)-phenyl propionic acid in N,N-Dimethyl formamide (DMF) respectively. Further they are subject to constant stirring for 12 h at ambient temperature of 30 °C till a precipitate in a dense solution is formed. The white crystalline crude complexes so obtained by removing excess DMF are then recrystallized with Dimethyl Sulfoxide (DMSO) and the yield varied from 85% to 95%. Yield of higher homologous complexes are observed to be more compared to its lower counterparts. The molecular structure of the present homologous series of p-n-alkoxybenzoic acids with (S)-1, 2–cholo-3-(4-hydroxy) phenyl propionic acid is depicted in the Scheme 1, where *n* represents the alkoxy carbon number while the molecular structure of the present ferroelectric hydrogen bonded complex is shown as Fig. 1.

3. Results and discussion

Hydrogen bonded ferroelectric liquid crystals (HBFLC) synthesized are white crystalline solids and are highly stable at ambient temperature (30°C). They are insoluble in water and sparingly soluble in common organic solvents such as methanol, ethanol, and benzene and dichloro methane. However, they show a high degree of solubility in coordinating solvents like Dimethyl Sulfoxide (DMSO), Dimethyl formamide (DMF) and Pyridine. Further the present HBFLC compounds melt at specific temperatures below 150 °C (Table 1). They show high thermal and chemical stability when subjected to repeated thermal scans performed during polarizing optical microscopic (POM) and DSC studies.

3.1. Phase identification

The observed phase variants, transition temperatures and corresponding enthalpy values obtained by DSC in cooling and heating cycles for the CTy + 8BA and CTy + 9BA complexes are presented in Table 1.

3.2. Polarizing optical microscopic studies (POM)

The hydrogen bonded complexes of the (S)-1,2–cholo-3-(4-hydroxy)phenyl propionic acid and alkoxy benzoic acid (CTy + *n*BA) are found to exhibit characteristic textures [31], viz., Nematic (N) (droplets), Smectic C* (broken focal conic texture) and Smectic G* (multi colored mosaic texture) respectively. The general phase sequence of the present ferroelectric hydrogen bonded complexes (viz. CTy + *n*BA where $n = 8$ and 9) in the cooling run are observed as:

Isotropic → N → SmC^* → SmG^* → Crystal (CTy+8BA)

Isotropic → N → N^* → SmC^* → SmG^* → Crystal (CTy+9BA)

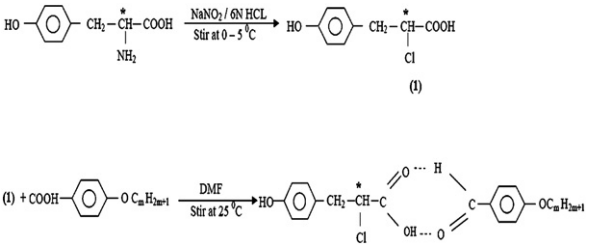

Scheme 1. Synthesis route of CTy + *n*BA inter hydrogen bonded liquid crystals.

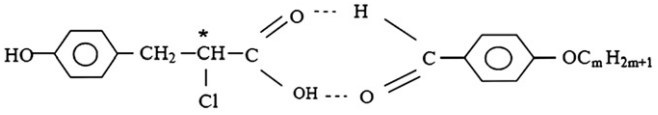

Fig. 1. Molecular structure of CTy + *n*BA inter hydrogen bonded complex.

Author's personal copy

Table 1
Comparison of transition temperatures (°C) obtained by various techniques. Enthalpy values (J/g) are given in parenthesis.

Carbon	Phase variance	Technique	Crystal-melt	N	N*	C*	G*	Crystal
8	NC*G*	DSC (h)	75.8 (27.74)	#		99.7 (1.63)	88.4 (0.39)	
		DSC (c)		119 (0.27)		92.4 (2.45)	77.9 (1.82)	52.1 (22.22)
		POM (c)		119.5		92.9	80.3	52.6
9	NN*C*G*	DSC (h)	94.5 (51.49)	#	126.9 (2.06)	116.2 (2.41)	#	
		DSC (c)		139.5 (10.78)	125.9 (0.18)	112.5 (1.31)	87.4 (15.72)	63.9 (33.96)
		POM (c)		139.9	126.4	112.6	87.9	64.4

monotropic transition, (h) heating cycle, (c) coolong cycle.

3.3. Infrared spectroscopy (FTIR)

IR spectra of pure p-n-alkoxybenzoic acid, (S)-1, 2–cholo-3-(4-hydroxy) phenyl propionic acid and their intermolecular H-bonded ferroelectric complexes were recorded in the solid state (KBr) at room temperature. Fig. 2 illustrates the FTIR spectra of the hydrogen bonded complex of CTy + 8BA in solid state at room temperature as a representative case. The solid state spectra of free alkoxybenzoic acid is reported [21] to have two sharp bands at 1685 cm^{-1} and 1695 cm^{-1} due to the frequency ν(C═O) mode. The doubling feature of this stretching mode confirms the dimeric nature of alkoxybenzoic acid at room temperature [21]. Further in the present hydrogen bonded complex a band appearing at 2928 cm^{-1} is assigned to ν(O–H) mode of the carboxylic acid group. Moreover, in the present hydrogen bonded complex, a sharp intense band at 768 cm^{-1} is attributed to the ν(C–Cl) stretching mode.

The doubling nature of ν(C═O) mode may be attributed to the dimeric nature of acid group at room temperature [21]. Corresponding spectrum of solution state (chloroform) shows a strong intense band suggesting the existence of monomeric form of benzoic acid. A noteworthy feature in the spectra of the present complex is the appearance of the sharp band at 1254 cm^{-1} and non appearance of the doubling nature of ν(C═O) mode of benzoic acid moiety. This clearly suggests that the dimeric nature of the benzoic acid dissociates and prefers to exist in a monomeric form upon complexation.

3.4. DSC studies

The phase transition temperatures and enthalpy values of CTy + 9BA (viz decyloxy benzoic acid with (S)-1,2–cholo-3-(4-hydroxy)phenyl propionic acid) is discussed as a representative case. Fig. 3 illustrates the thermo gram of CTy + 9BA hydrogen bonded complex recorded at a scan rate of 10 °C/min for the heating and cooling runs. In the cooling run of DSC thermo gram the above compound possesses five distinct transitions namely isotropic to Nematic, Nematic to N*, N* to Sm C*, Sm C* to Sm G* and Sm G* to crystal with transition temperatures 139.5 °C, 125.9 °C, 112.5 °C, 87.4 °C and 63.9 °C with corresponding enthalpy values 10.78 J/g, 0.18 J/g, 1.31 J/g, 15.72 J/g, and 33.96 J/g respectively. While in the heating cycle three distant transitions namely crystal to melt, N to N* and N* to Sm C* are obtained at 94.5 °C, 126.92 °C and 116.2 °C with corresponding enthalpy values of 51.49 J/g, 2.06 J/g and 2.41 J/g respectively. Phase transitions in the DSC heating scan corresponding to melt to N and Sm C* to Sm G* of CTy + 9BA are observed to be monotropic. Similarly the phase transition in the DSC heating scan corresponding to melt to nematic of CTy + 8BA is observed to be monotropic.

The transition temperatures and enthalpy values for CTy + 8BA and CTy + 9BA hydrogen bonded ferroelectric complex are analyzed and presented in Table 1. All these transition temperatures of the present homologous series concur with data obtained from POM studies.

3.5. Phase diagrams

3.5.1. Phase diagram of pure p-n-alkoxybenzoic acids

The phase diagrams of pure p-n-alkoxybenzoic acids is reported [24] while the present hydrogen bonded ferroelectric homologous series is constructed through POM studies and by the phase

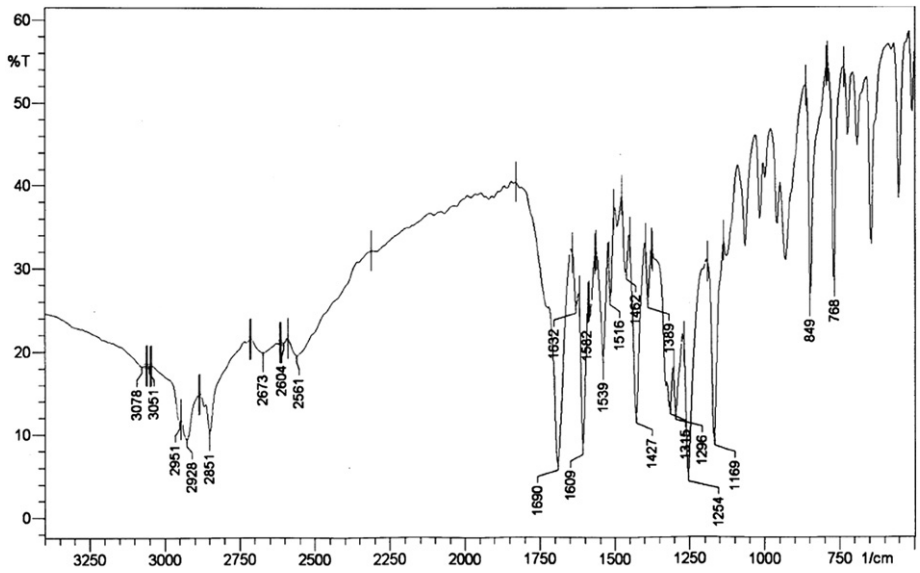

Fig. 2. FTIR spectra of CTy + 8BA inter hydrogen bonded complex.

Author's personal copy

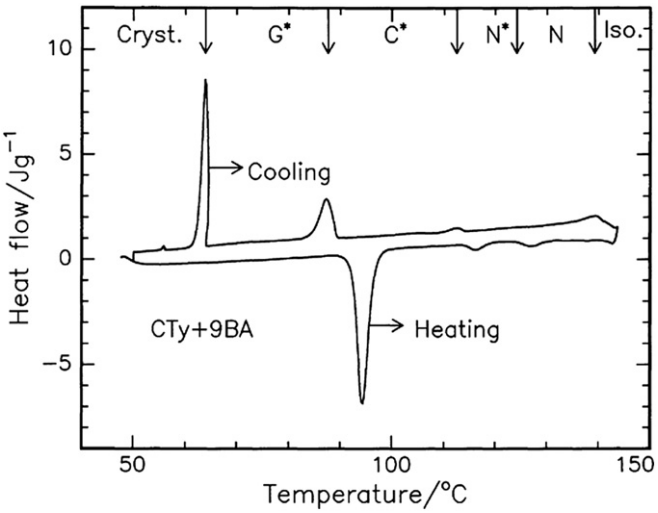

Fig. 3. DSC thermo gram of CTy + 9BA inter hydrogen bonded complex.

transition temperatures observed in the cooling run of the DSC studies. The phase diagram of pure p-n-alkoxybenzoic acid is reported [24] to composed of three phases namely, Nematic, smectic C* and smectic G*.

3.5.2. Phase diagram of CTy + nBA homologous series

The phase diagram of the present hydrogen bonded ferroelectric homologous series is depicted in Fig. 4. The following points can be observed from the Fig. 4

a) Mesogenic thermal range gradually increased with increment in the alkoxy carbon number from pentyloxy to dodecyloxy benzoic acid.
b) The homologous series exhibits rich phase abundance, the number of phases exhibited by the individual member's increases as the carbon number is increased up to nonyloxy benzoic acid.
c) In the last three members of the series, namely decyloxy, undecyloxy; and dodecyloxy benzoic acids, the phase variance stabilized to three phases viz, N, smectic C* and smectic G*.
d) A new phase namely N* is found to induce in the one member of the homologous series.

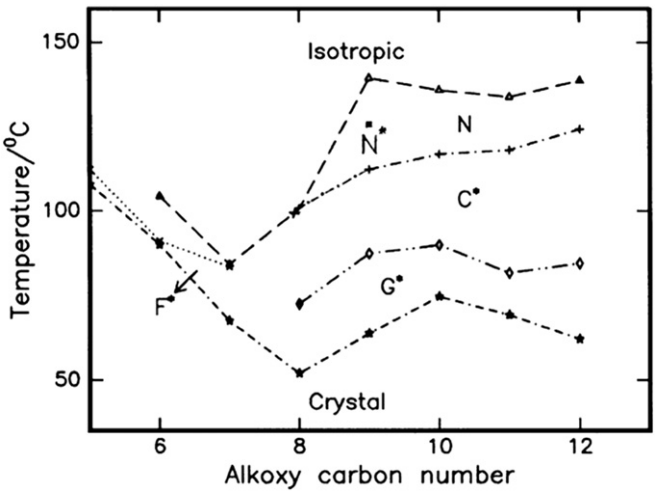

Fig. 4. Phase diagram of CTy + *n*BA homologous series.

e) Apart form the distinguishable textural differences, the phase N switches with the applied electric stimulus while N* is unswitchable.
f) In the lower homologous members of the series, smectic F* is found to be pronounced while in the higher homologous members of the series smectic G* is pronounced.
g) Compared to the pure benzoic acids, in the present hydrogen bonded complex the thermal span of the three main phases viz., nematic, smectic C* and G* are found to be almost equal to one another.

3.6. Field induced transition (FiT)

It is earlier reported [29,32–40] that when a chiral compound is subjected to an applied external dc stimulus in nematic phase, there can be a phase transition which is referred as Field induced Transition (FiT). The present hydrogen bonded homologous compounds are subjected to various strengths of external dc electric stimulus derived from HP 4192A impedance analyzer to investigate the occurrence of FiT. In CTy + 8BA compound in its nematic phase, four new field induced phases (FiT) referred as, E_1, E_2, E_3 and E_4 are identified.

3.7. FiT in CTy + 8 BA in nematic phase

CTy + 8BA compound in its nematic phase when an applied dc stimulus exceeds a particular threshold values, the phases of the compound is observed to change which are referred as field induced transitions (FiT). These transitions are classified as E_0, E_1, E_2, E_3 and E_4 respectively. Each of these induced phases possesses different characteristic texture and threshold voltage levels. It is worth mentioning that in any of the phase when the external field is withdrawn, immediately the original nematic texture is observed. Thus all these field induced transitions are reversible. In the nematic phase the field induced transitions observed along with the threshold field values are given below:

$$E_0^{0\le 1.25V/\mu} \rightarrow E_1^{1.26\le 2.24V/\mu} \rightarrow E_2^{2.25\le 3.49V/\mu} \rightarrow E_3^{3.50\le 4.99V/\mu} \rightarrow E_4^{\ge 5V/\mu}$$

3.7.1. E_0 phase ($0 \le 1.25V/\mu$)

When an external dc stimulus field is between 0 and 1.25 volts/micron there is no change in the threaded nematic texture. This phase is designated as E_0 phase (Plate 1a). The external stimulus could not change the texture perhaps due to the strong surface anchoring energy between the liquid crystal and the substrate. In addition the inter molecular forces play a pivotal role in preventing the external stimulus to disturb the given orientation of the molecules. In the texture, the intensity of light in entire span of this phase remains constant as shown in Fig. 5. Magnitude of helix in this phase remains constant as can be observed from Fig. 6.

3.7.2. E_1 phase ($1.26V/\mu \le 2.24V/\mu$)

A sudden change in the texture of the nematic phase as depicted in Plate 1b is observed when the external stimulus field attains a threshold value of 1.26 V/μ. A new texture called as worm like texture is observed and this phase is labeled as E_1 phase. The texture persists till the external field reaches a threshold value of 2.24 V/μ. It is believed that the external stimulus given to the molecules enabled them to partially overcome the surface anchoring energy, thus the molecules are realigned themselves forming a new worm like texture. From Fig. 5 it can be observed

Author's personal copy

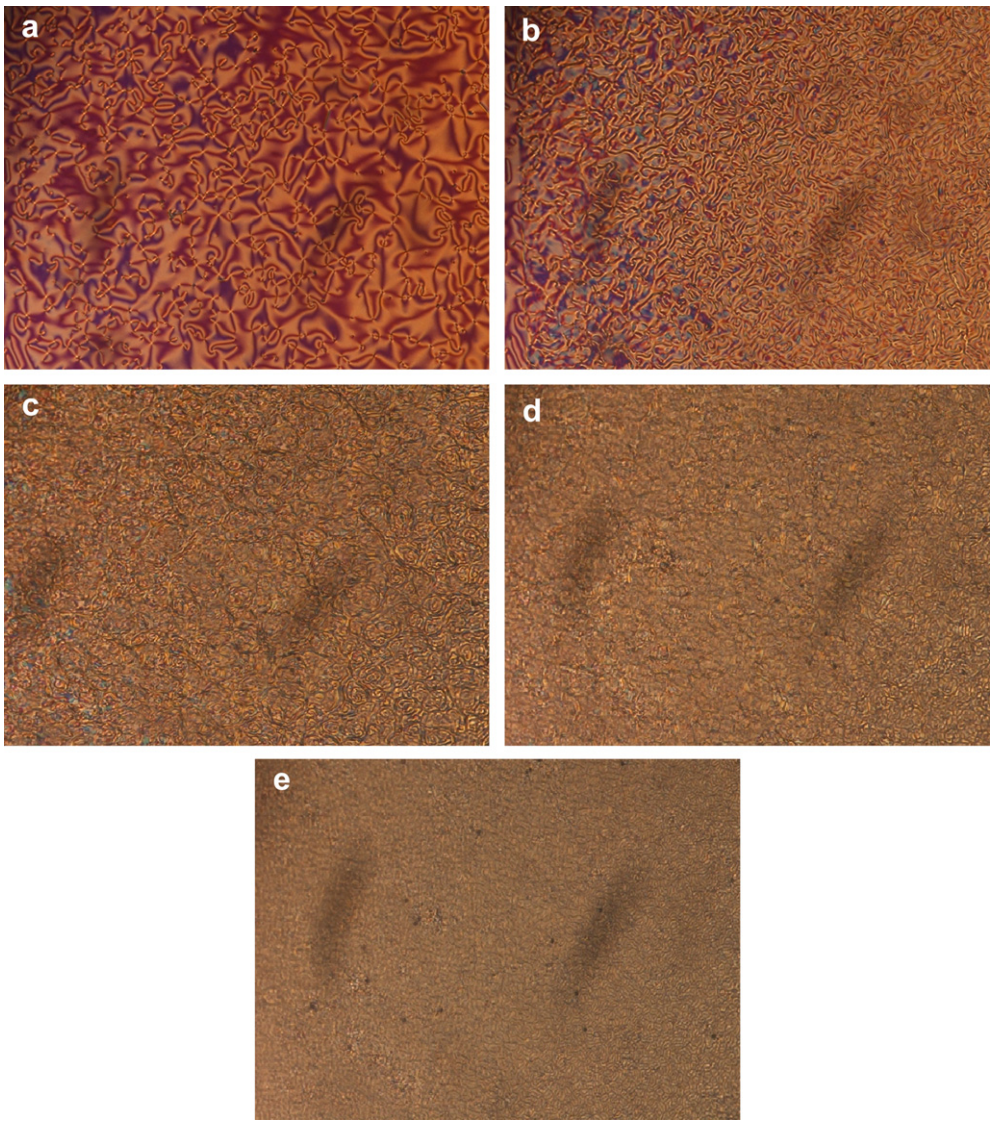

Plate 1. a. Nematic texture with an applied external field range of $0 \leq 1.25$ V/μ. This phase is designated as E_0 phase. b. Worm like texture with an applied external field range of 1.26 V/μ ≤ 2.24 V/μ and the phase is designated as E_1 phase. c. Sandy texture with an applied external field range of 2.25 V/μ ≤ 3.49 V/μ and the phase is designated as E_2 phase. d. Grain type texture with an applied external field range of 3.50 V/μ ≤ 4.99 V/μ and the phase is designated as E_3 phase. e. Cluster type texture with an applied external field range of ≥ 5.0 V/μ and the phase is designated as E_4 phase.

that the light intensity decreases in this phase when compared to E_0 phase, further it can be noted that as the field increases, the molecules prefer an alignment which inhibits the light. Deformation of helix is one of the reasons for the existence of this phase, which has been confirmed by the Fig. 6. The magnitude of helix decreased with the onset of this phase and remains constant in the entire span of E_1 phase.

3.7.3. E_2 phase (2.25V/μ ≤ 3.49V/μ)

When the external field reaches a threshold value of 2.25 V/μ, there is yet another field induced transition which is labeled as E_2 phase. A sandy texture (Plate 1c) is observed in this phase and the same texture persists till 3.49 V/μ. The external stimulus given to the molecules enabled to completely overcome the surface anchoring energy. Thus in this phase the molecules have more degrees of freedom. A steep decrement in the light intensity is observed in this phase (Fig. 5). The magnitude of helix further decreased with the onset of this phase and remains constant in the entire E_2 phase (Fig. 6).

3.7.4. E_3 phase (3.50V/μ ≤ 4.99V/μ)

When the external field reaches a threshold value of 3.50 V/μ, there is yet another field induced transition which is labeled as E_3 phase. In this phase the molecules are aggregated and a grain type texture (Plate 1d) is observed and the same texture persists till 4.99 V/μ. In addition to the surface anchoring energy the inter molecular association will be extremely weak. Thus in this phase the molecules possess more rotation. As a result the magnitude of the light intensity is considerably reduced (Fig. 5). This is also manifested in the steep decrement of the magnitude of helix (Fig. 6). Thus the deformation of helix coupled with weak binding of the molecules results in E_3 phase.

3.7.5. E_4 phase (≥ 5.0V/μ)

A sudden change in the texture of the phase as depicted in Plate 1e is observed when the external stimulus field attains a threshold value of 5.0 V/μ. A new texture named as thick cluster type texture is observed and this phase is labeled as E_4 phase. This texture persists even after the external stimulus is further increased. The

Author's personal copy

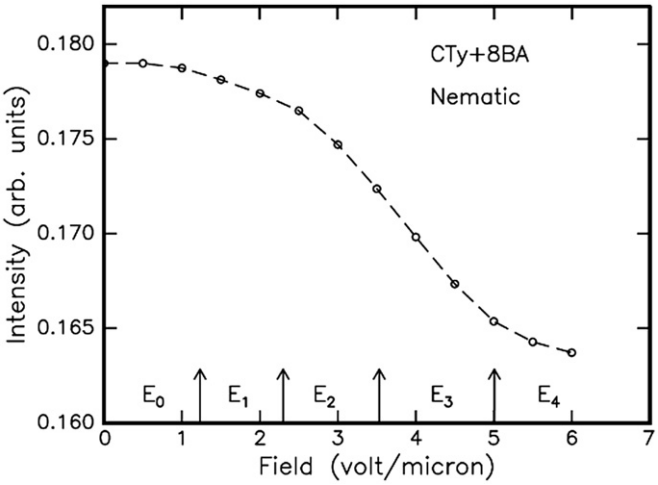

Fig. 5. Intensity profile variation with applied stimulus.

helix is almost deformed as depicted in Fig. 6. As a consequence the light intensity also rapidly falls off which can be evinced from Fig. 5. The molecules are highly agitated with the high external field and thus align in such a position which hinders the light. The light modulation is clearly observed.

3.8. Variation of capacitance with applied field

A study of capacitance with applied voltage has been investigated and plotted as Fig. 7. From the Fig. 7 the following points can be noted

a) Field induced transitions i.e. $E_0 - E_1$, $E_1 - E_2$, $E_2 - E_3$ and $E_3 - E_4$ are observed to be not sudden and abrupt but smooth and uniform.
b) There exits a threshold voltage value which even can be detected by the variation of the capacitance, above these threshold voltages the capacitance increases linearly indicating the occurrence of new induced phases due to FiT.
c) The equilibrium states for the low and the high field are found to be distinct.

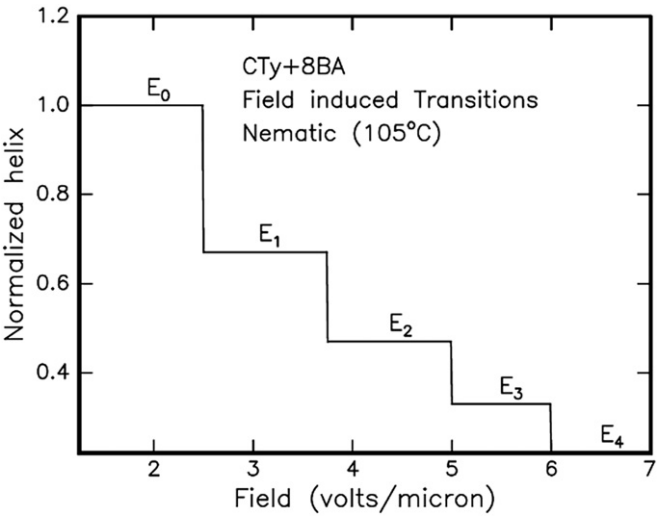

Fig. 6. Helical pitch variation in various FiT with applied field in nematic phase of CTy + 8BA hydrogen bonded complex.

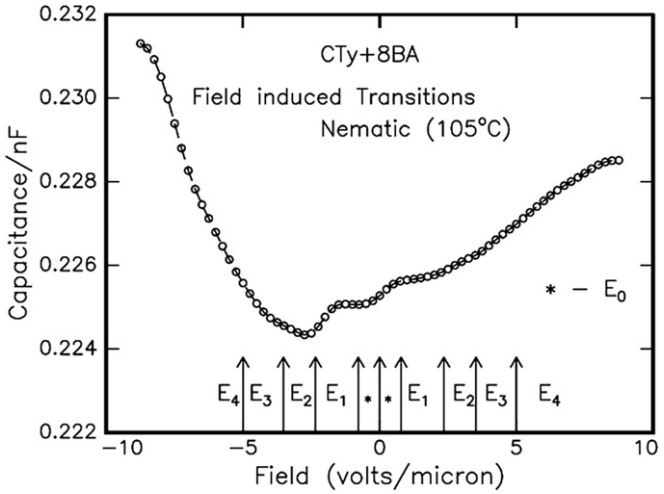

Fig. 7. Capacitance variation in various FiT with applied field in nematic phase of CTy + 8BA complex.

d) The shape of the curve obtained with capacitance is unaltered at all frequencies implying that frequency has little or no impact on all the observed field induced transitions.

3.9. Dielectric hysteresis

The primary requisite for any liquid crystalline materials to be used in device applications is possessing of a tilted phase and presence of any type of hysteresis. In the present study, along with the field induced transitions, another interesting observation is the detection of appearance of dielectric hysteresis in one of the compound.

Dielectric studies are performed on CTy + 8BA compound in its nematic phase. To detect dielectric hysteresis, data of capacitance along with dielectric loss are plotted for various fields varying from 0 volts/micron to 8.75 volts/micron and retracing the voltage path from 8.75 volts/micron to 0 volts/micron in steps of 0.5 volts/micron respectively. Data of capacitance and dielectric loss so obtained are plotted in Figs. 8 and 9 respectively. It can be seen that in both the figures, a noticeable dielectric hysteresis loop is observed indicating the memory capability of the liquid crystal under study. The area under the curve in both the capacitance and

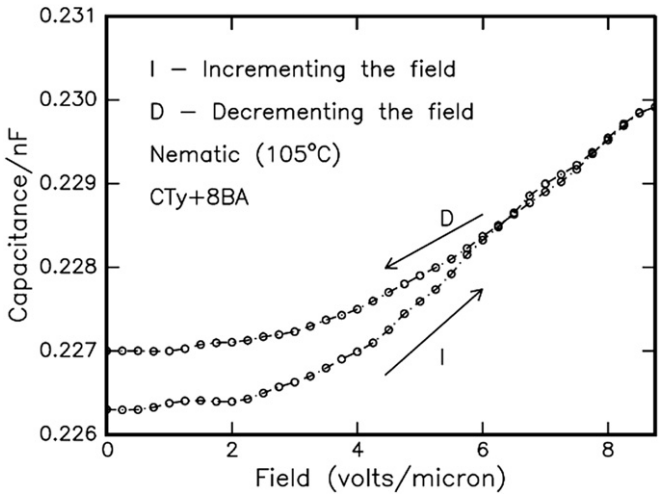

Fig. 8. Hysteresis plot of capacitance in nematic phase of CTy + 8BA.

Author's personal copy

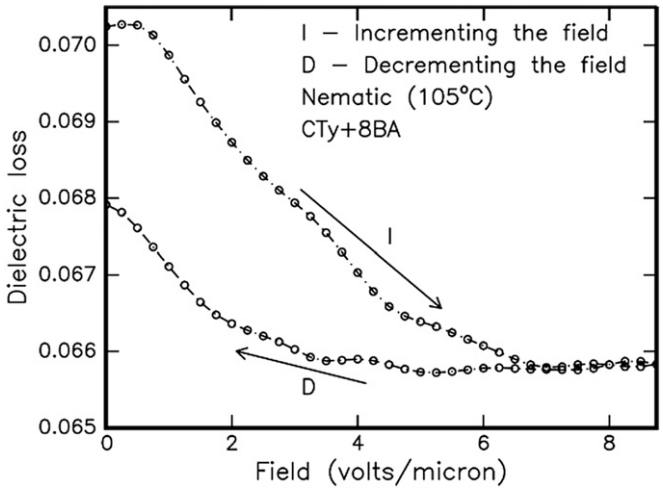

Fig. 9. Hysteresis plot of dielectric loss in nematic phase of CTy + 8BA.

dielectric loss experiments are observed to be almost identical. This indicates that an identical process is taking place at the ferroelectric domain level in both the dielectric measurement techniques. Fig. 10 illustrates the field variation of hysteresis loop width for capacitance and dielectric loss in nematic phase at 105 °C for CTy + 8BA hydrogen bonded complex. The trend of variation in both the cases is observed to be similar indicating the same type of mechanism involved in both the processes. The gradual decrement of the hysteresis loop width is observed with increasing magnitude of external field. No anomalies are found at threshold values of the field induced transitions. Thus the FiT has no significant contribution towards the magnitude of hysteresis. At a threshold field value of 8 volts/micron the hysteresis loop is observed to be zero while the maximum value of the loop is observed at zero field. Thus the sample under investigation possesses the retentivity capability in terms of dielectric data.

4. Optical tilt angle studies in smectic C*

Optical tilt angle has been experimentally measured by optical extinction method [41] in the smectic C* phase of CTy + 8BA. From the Fig. 11, it is observed that the magnitude of the tilt angle

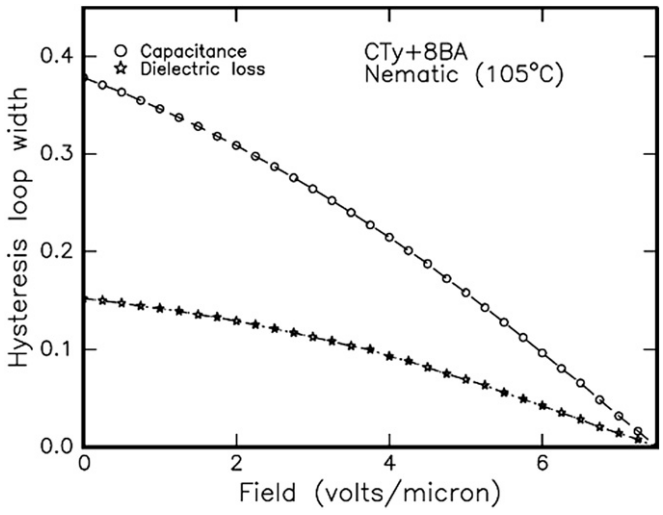

Fig. 10. Hysteresis loop width plot for dielectric parameters of CTy + 8BA.

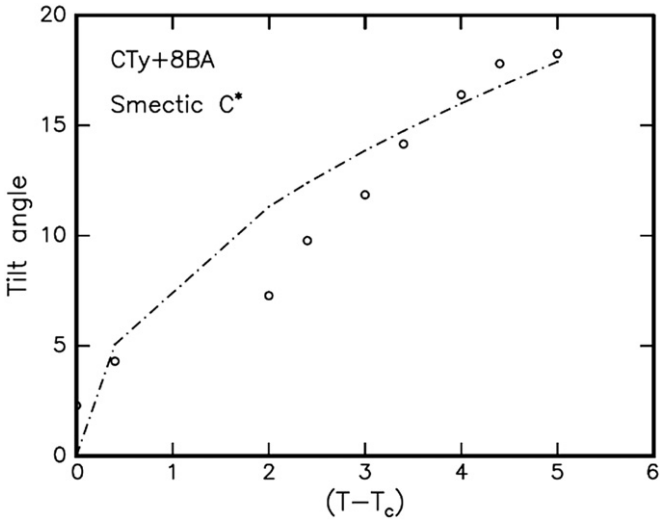

Fig. 11. Temperature variation of tilt angle in smectic C* phase of CTy + 8BA. Dotted line denotes the power law fit.

increases with decreasing temperature and attains a saturation value. The saturated value of the tilt angle in smectic C* of CTy + 8BA is observed to be ~18° The large magnitudes of the tilt angle are attributed [22] to the direction of the soft covalent hydrogen bond interaction which spreads along molecular long axis with finite inclination.

Tilt angle is a primary order parameter [42,43] in ferroelectric phase viz smectic C* and the temperature variation is estimated by fitting the observed data of θ (T) to the relation

$$\theta(T)\alpha(T - T_C)^{\beta} \quad (1)$$

The critical exponent β value estimated by fitting the data of θ (T) to the above equation (1) is found to be 0.50 which agrees with the Mean Field [43] prediction. The dotted line in the Fig. 11 depicts the fitted data. Further, the agreement of β with Mean Field value infers the long–range interaction of transverse dipole moment for the stabilization of tilted smectic C* and FiT smectic ordering phases.

5. Field effect on helicoidal structure

In the literature it is reported [44–50] the distortion and unwinding of the helicoidal structure with applied field in the liquid crystal mesogen yield field induced transitions (FiT). The untwisting of the helical structure in the present complexes filled in a thin plane layer exposed to an external action (temperature or field) and its dependence on the molecular adhesive forces at the layer boundaries are studied.

In the present work, the helical pitch is measured by diffraction of He–Ne red laser light on liquid crystal sample filled in a commercial available (Instec) buffed conducting cell. This method can be used for measurement of the helical pitch of short length. The present compound of CTy + 8BA is filled in such a commercially available cell and silver leads are drawn for contact. The deformation of the helicoidal structure has been experimentally analyzed by applying external variable bias voltage (0 to ±35 V) drawn from impedance analyzer at various frequencies. As the external voltage is incremented in small steps, this in turn induced various FiT at different magnitudes of the applied voltage. The variation of the helix is noted at each step of the applied field. It is not surprising to note that the magnitude of the helix is unaltered in between any

Author's personal copy

threshold field values of respective FiT but drastically varies at the induced transitions namely E_0, E_1, E_2, E_3 and E_4 respectively as represented in Fig. 6. At all the field induced transitions there is a step like sudden decrement of the magnitude of helix manifesting the distortion of the helix as shown in Fig. 6. It is pertinent to mention that the intensity of the light profile from the liquid crystal cell under crossed polarizer gradually decreased and in the final FiT phase the liquid crystal behaved as a light modulator (Plate 1a–e). Hence these HBFLC materials may be used as light modulators.

6. Conclusions

a) Novel hydrogen bonded ferroelectric liquid crystal series has been synthesized and characterized.
b) The formation of hydrogen bond is conformed by FTIR measurements.
c) A detailed analysis of various field induced transitions in nematic phase of one of the hydrogen bonded complex is performed.
d) Dielectric data, optical studies and helix measurements supported the observed field induced transitions.
e) Dielectric hysteresis is observed and characterized for one hydrogen bonded complex.

Acknowledgements

One of the authors (MLNMM) acknowledges the financial support rendered by All India Council for Technical Education (AICTE), Department of Science and Technology (DST), and Defense Research Development Organization (DRDO) New Delhi. Infrastructural support provided by Bannari Amman Institute of Technology is gratefully acknowledged.

References

[1] T. Kato, J.M.J. Frechet, J. Am. Chem. Soc. 111 (1989) 8533.
[2] (a) U. Kumar, T. Kato, J.M.J. Frechet, J. Am. Chem. Soc. 114 (1992) 6630;
(b) A. Sato, T. Kato, T. Uryu, J. Polym. Sci. Part. A Poly. Chem. 34 (1996) 503;
(c) T. Kato, J.M.J. Frechet, P.G. Wilson, T. Saito, T. Uryu, A. Fujishima, C. Jin, F. Kaneuchi, Chem. Mater. 5 (1993) 1094;
(d) T. Kato, H. Kihara, T. Uryu, A. Fujishima, J.M.J. Frechet, Macromolecules 25 (1992) 6836;
(e) T. Kato, Handbook of Liquid Crystals. Wiley-VCH, Weinheim, 1998.
[3] G.W. Gray, Molecular Structure and Properties of Liquid Crystals. Academic Press, London, 1962.
[4] H. Kelker, R. Hatz, Handbook of Liquid Crystals. Verlag Chemie, Weinheim, 1980.
[5] R.B. Meyer, L. Liebert, L. Strezelecki, P. Keller, J. Physique. Lett. 30 (1975) 69.
[6] L. Yu, Liq. Cryst. 14 (1993) 1303.
[7] (a) T. Kato, H. Kihara, T. Uryu, S. Ujiie, K. Iimura, J.M.J. Frechet, U. Kumar, Ferroelectrics 148 (1993) 161;
(b) T. Kato, M. Nakano, T. Moteri, T. Uryu, S. Ujiie, Marcomolecules 28 (1995) 8875;
(c) T. Kato, Kor. Poly. J. 4 (1996) 125;
(d) T. Kato, J.M.J. Frechet, Macromolecules 22 (1989) 3818;
(e) U. umar, J.M.J. Frechet, T. Kato, S. Ujiie, K. Iimura, Angew. Chem. Int. Ed. Engl. 31 (1992) 1531.
[8] (a) T. Kato, T. Uryu, F. Kaneuchi, C. Jin, J.M.J. Frechet, Liq. Cryst. 14 (1993) 1311;
(b) T. Kato, N. Hirota, A. Fujishima, J.M.J. Frechet, J. Polym. Sci. Part. A Poly. Chem. 34 (1996) 57;
(c) T. Kato, H. Kihira, U. Kumar, T. Uryu, J.M.J. Frechet, Angew. Chem. Int. Ed. Engl. 33 (1994) 1644;
(d) H. Kihara, T. Kato, T. Uryu, J.M.J. Frechet, Chem. Mater. 8 (1996) 961.
[9] D. Demus, H. Demus, H. Zaschke, Flussige Kristalle in Tabellen. VEB Deutcher Verlag fur Grundstoffindustrie, Leipzig, 1974.
[10] C.M. Paleos, D. Tsiourvas, Liq. Cryst. 28 (2001) 1127.
[11] B. Xu, T.M. Swager, J. Am. Chem. Soc. 117 (1995) 5011.
[12] S. Malik, P.K. Dhal, R.A. Mashelkar, Macromolecules 28 (1995) 2159.
[13] Z. Sideratou, D. Tsiourvas, C.M. Paleos, A. Skoulios, Liq. Cryst. 22 (1997) 51.
[14] J.W.D. Goodby, R. Blinc, N.A. Clark, S.T. Lagerwall, S.A. Osipov, S.A. Pikin, T. Sakurai, Y. Yoshino, B. Zecks, Ferro Electric Liquid Crystal, Principles, Properties and Applications. U.S.A.Gorden and Breech Press, Philadalphia, 1991.
[15] N.A. Clark, S.T. Lagerwall, Appl. Phys. Lett. 36 (1980) 899.
[16] H.R. Brand, P.E. Cladis, H. Pleiner, Macromolecules 25 (1992) 7223.
[17] M.P. Petrov, L.V. Tsonev, Liq. Cryst. 21 (1996) 543.
[18] P.A. Kumar, M. Srinivasulu, V.G.K.M. Pisipati, Liq. Cryst. 26 (1999) 859.
[19] P. Swathi, P.A. Kumar, V.G.K.M. Pisipati, Liq. Cryst. 27 (2000) 665.
[20] M. Srinivasulu, P.V.V. Satyanarayana, P.A. Kumar, V.G.K.M. Pisipati, Liq. Cryst. 28 (2001) 1321.
[21] P. Swathi, S. Sreehari Sastry, P.A. Kumar, V.G.K.M. Pisipati, Mol. Cryst. Liq. Cryst. 365 (2001) 523.
[22] B. Sreedevi, P.V. Chalapathi, M. Srinivasulu, V.G.K.M. Pisipati, D.M. Potukuchi, Liq. Cryst. 31 (2004) 303.
[23] T. Chitravel, M.L.N. Madhu Mohan, V. Krishnakumar, Mol. Cryst. Liq. Cryst. 493 (2008) 17.
[24] V.N. Vijayakumar, K. Murugadass, M.L.N. Madhu Mohan, Mol. Cryst. Liq. Cryst. 515 (2009) 37.
[25] (a) M.L.N. Madhu Mohan, B. Arunachalam, C. Arravindh Sankar, Metal. Mater. Trans. A 39 (2008) 1192;
(b) M.L.N. Madhu Mohan, B. Arunachalam, Z. Naturforch 63a (2008) 435.
[26] M.L.N. Madhu Mohan, V.G.K.M. Pisipati, Liq. Cryst. 26 (2000) 1609.
[27] (a) P.A. Kumar, M.L.N. Madhu Mohan, V.G.K.M. Pisipati, Liq. Cryst. 27 (2000) 1533;
(b) M.L.N. Madhu Mohan, P.A. Kumar, B.V.S. Goud, V.G.K.M. Pisipati, Mater. Res. Bull. 34 (1999) 2167.
[28] (a) M.L.N. Madhu Mohan, P.A. Kumar, V.G.K.M. Pisipati, Ferroelectrics 227 (1999) 105;
(b) M.L.N. Madhu Mohan, D.M. Potukuchi, V.G.K.M. Pisipati, Mol. Cryst. Liq. Cryst. 325 (1998) 127.
[29] (a) V.N. Vijayakumar, M.L.N. Madhu Mohan, Ferroelectrics 392 (2009) 81;
(b) V.N. Vijayakumar, M.L.N. Madhu Mohan, Solid State Commun. 149 (2009) 2090.
[30] (a) V.N. Vijayakumar, K. Murugadass, M.L.N. Madhu Mohan, Braz. J. Phys. vol. 39 (2009) 600;
(b) V.N. Vijayakumar, K. Murugadass, M. L.N. Madhu Mohan, Molecular Crystals and Liquid Crystals, 515 (2009) 37.
[31] G.W. Gray, J.W.G. Goodby, Smetic Liquid Crystals–Textures and Structures, London: Leonard Hill, 1984.
[32] S. Kobayashi, S. Ishibashi, Mol. Cryst. Liq. Cryst. 257 (1994) 181.
[33] W. Jong-Guang, C. Shu-Hsia, Jpn. J. Appl. Phys. 33 (1994) 6249.
[34] T. Qian, P.L. Taylor, Phys. Rev. E 60 (1999) 2978.
[35] G. Napoli, J. Appl. Maths 71 (2006) 34.
[36] L.J.M. Schlangen, P. Alexandre, H.J. Cornelissen, J. Appl. Phys. 87 (2000) 3723.
[37] A.J. Hurd, S. Fraden, F. Lonberg, R.B. Meyer, J. de Physique 46 (1985) 905.
[38] S. Zhang, B. Wen, S.S. Keast, M.E. Neubert, P.L. Taylor, C. Rosenblatt, Phys. Rev. Lett. 84 (2000) 4140.
[39] T.A. Rotinyan, E.I. Ryumtsev, S.B. Yazikov, JETP Lett. 46 (1987) 417.
[40] P.E. Cladiss, T. Garel, P. Pieranski, Phys. Rev. Lett. 57 (1986) 2841.
[41] C. Noot, S.P. Perkins, H.J. Coles, Ferroelectrics 244 (2000) 331.
[42] P.G. de Gennes, The Physics of Liquid Crystals. Oxford Press, London, 1974.
[43] H.E. Stanley, Introduction to Phase Transition and Critical Phenomena. Clarendon Press, 1971.
[44] M. Petit, A. Daoudi, M. Ismaili, J.M. Buisine, Eur. Phys. J. E. Soft. Matter 20 (2006) 327.
[45] I. Abdulhalim, G. Moddel, Mol. Cryst. Liq. Cryst. 200 (1991) 79.
[46] L.A. Judge, E.E. Kriezis, S.J. Elston, Mol. Cryst. Liq. Cryst. 366 (2001) 661.
[47] P. Schiller, F. Zeitler, Phys. Rev. E 56 (1997) 531.
[48] P. Schiller, F. Zeitler, J. de Physique II 5 (1995) 1835.
[49] B.Y. Zeldovich, N.V. Tabiryan, JETP Lett. 34 (1981) 428.
[50] V.A. Belyakov, JETP Lett. 76 (2002) 88.